FINITE ELEMENT ANALYSIS OF UHPFRC PLATES UNDER IMPACT LOADS

Hesham Othman (1) and Hesham Marzouk (1)

(1) Department of Civil Engineering, Ryerson University, Toronto, Canada

Abstract

A three-dimensional finite element analysis has been conducted to model multi-impacts on UHPFRC plates that were previously tested by the authors. A brief description of the experimental tests is provided. The numerical simulation has been performed using ABAQUS/Explicit. Concrete and reinforcing steel are represented by separate material models which are combined together to describe the behaviour of the composite RC material. Concrete Damage Plasticity (CDP) model is adapted to define UHPFRC material. The objective of this research is to assess whether the existing CDP constitutive model with adjustable parameters may be able to accurately replicate the dynamic response of UHPFRC member. Computed responses are sensitive to CDP parameters related to the tension, fracture energy, and expansion properties. The analytical results showed that the existing CDP model can predict the response and crack pattern of UHPFRC reasonably well. Instabilities of results were observed in the impact analyses that corresponding to extensive damage level of fibers bridging action stage.

Résumé

Une analyse tridimensionnelle aux éléments finis a été menée pour modéliser les impacts successifs sur des dalles de BFUP préalablement testées par les auteurs. Une brève description des essais est fournie. La simulation numérique a été faite avec ABAQUS/Explicit. Le béton et les armatures sont représentés par des matériaux séparés dont la combinaison permet de décrire le comportement du composite béton armé. Un modèle de plasticité avec endommagement pour le béton a été adapté pour décrire le BFUP. L'objectif de la recherche est de vérifier si ce modèle de comportement existant, moyennant l'ajustement des paramètres, peut représenter précisément le comportement dynamique d'un élément en BFUP. Les résultats de calcul sont sensibles aux paramètres décrivant la traction, à l'énergie de rupture et aux propriétés d'expansion. Les résultats analytiques montrent que le modèle de plasticité avec endommagement pour le béton peut prédire assez bien la réponse et le faciès de fissuration du BFUP. Les instabilités observées dans les analyses d'impact correspondent à un stade d'endommagement généralisé associé à la contribution des fibres.

1. INTRODUCTION

Ultra-high performance fiber reinforced concrete (UHPFRC) is a relatively new cementitious material consisting of an optimum combination of cement, fine sand, silica fume, superplasticizer, water, and fibers. UHPFRC has been developed to improve the mechanical and/or durability properties of concrete. Such properties include: ultra-compressive strength exceeding 150 MPa, enhanced tensile strength in the range of 8-15 MPa, high elastic modulus, strain hardening in tension [1], and fracture energy of several orders of magnitudes of traditional concrete [2].

The demand for impact resistant design has a wide spectrum for many applications, such as offshore platform, rock sheds, protective structures, transportation structures, etc. UHPFRC has been identified as one of the promising ways to innovate in impact resistance structures. Despite the obvious advantage of UHPFRC mechanical and durability properties, its structural application is not very widespread. Lack of practical material constitutive model and well defined mathematical formulas to estimate material properties of UHPFRC are of the main reasons that limit the use of UHPFRC in practical engineering. Several investigations have shown that the mechanical properties of UHPFRC material are different from traditional concrete, in particular, the tensile response, fracture energy [2,3], and strain rate effects [4,5]. These differences in material behavior might result in more complexity to the finite element (FE) simulation of UHPFRC under impact loads. The main objective of this research is to assess if the existing CDP constitutive model with adjustable material parameters is able to predict the dynamic response of UHPFRC member. The FE analysis is performed using ABAQUS/Explicit, version 6.14 [6]. Explicit analysis is suitable for dynamic events with strong discontinuous geometrical and/or material responses.

2. EXPERIMENTAL PROGRAM

2.1 Test specimens

Three reinforced UHPFRC specimens with identical dimensions are tested under repeated drop-weight impact. The specimens have dimensions 1950×1950×100 mm. All specimens are doubly reinforced with equal top and bottom steel of 10M CSA re-bars of Grade 400 [7]. Steel reinforcement ratio (0.47, 0.64, and 1.00% per layer/direction) is varied amongst the three plates. A summary of the studied parameters is presented in Table 1. UHPFRC specimens are cast using a commercial product of Lafarge North America. All UHPFRC specimens are cast using same mix proportions with steel fiber content of 2 % by volume. This fiber content is recommended by the supplier and it is a commonly used percent in the industry. Short steel fibres with an aspect ratio of 65 (13/0.2 mm) are used.

Table 1: Details of test specimens

Specimen	Steel reinforcement (per layer)	
	Ratio*, (%)	Dai./spacing, (mm)
UH-S_{100}	1.00	10M/100
UH-S_{158}	0.64	10M/158
UH-S_{210}	0.47	10M/210

The measured geometrical and mechanical properties of UHPFRC and steel reinforcement are presented in Table 2. Static mechanical properties of UHPFRC are measured at the reference quasi-static strain rates recommended by CEB-FIP [8]. Additionally, the mechanical properties of UHPFRC are tested at different strain rates up to 4000 the reference quasi static rates to estimate the enhancement in UHPFRC properties. More details regarding strain rate effect on UHPFRC can be found in [5]. These properties are used as input for constitutive material models. The stress-strain relations at different strain rate are presented side by side with the adapted input stress-strain curves in constitutive modeling section.

Table 2: Reference quasi-static mechanical properties of concrete materials

Concrete	Density (kg/m^3)	Compressive strength f_c', (MPa)	Elastic modulus E_c, (GPa)	Flexural strength f_r, (MPa)	Splitting strength f_{tsp}, (MPa)
UHFRC	2650	162.4	48.8	19.2	11.1
Steel re-bar	Diameter (mm)	Mass (kg/m)	Elastic modulus E_s, (GPa)	Yield stress f_y, (MPa)	Ultimate strength f_{ult}, (MPa)
10M	11.29	0.775	201.10	433.40	621.70

2.2 Drop-weight impact testing

Figure 2 illustrates the drop-weight impact testing setup. All Specimens are tested under same boundary and loading conditions. Specimens are subjected to a drop-weight impact at the central point and supported at the four corners. A special steel frame is used to prevent uplift of specimen corner. The plates are tested under repeated drop-weight impact. The impact tests are applied by dropping 475 kg mass from a height of 4.15 m.

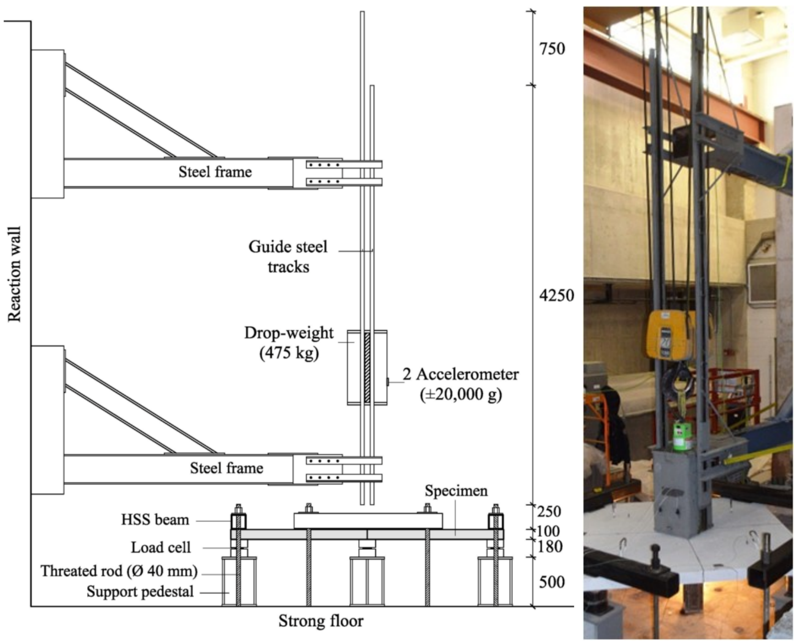

Figure 2: Drop-weight impact test (dimensions in mm) [9]

All specimens are subjected to seven drop-weight tests. The contact surface between the drop-weight and specimens is flat with dimensions of 400×400 mm. The impact setup is well-equipped with advanced instrumentation to monitor impact force, reaction forces at the four corners; midpoint displacement, and steel reinforcement strain at central zone. Additionally, the impact velocity is estimated using a high-speed camera. More details regarding the test setup, instrumentation, and experimental investigation results can be found in [9]. Experimental measurements are presented side by side with FE estimation in numerical results section.

3. NUMERICAL MODELING

3.1 Development of FE Model

Fig. 3 shows the generated geometry and boundary conditions of the specimen UH-S_{100}. Eight-node solid elements with reduced integration (C3D8R) are used to model concrete. Steel reinforcement is modeled using two-node beam element (B31). The embedded constraint is implemented to simulate the bond between steel reinforcement and concrete assuming perfect bond. The drop-weight and supporting system are modeled using eight-node solid elements with reduced integration (C3D8R). General contact interaction is used to define the contact between drop-weight and the specimen as well as between the specimen and the supporting systems. The hard contact is used to define the contact interaction in the normal direction. The drop-weight is modeled in an initial position close to the specimen surface with a pre-defined velocity equal to that extracted from the recorded video.

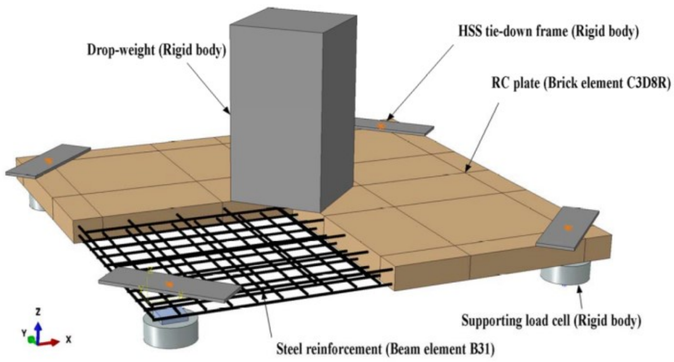

Figure 3: FE model of drop-weight impact test (specimen UH-S_{100})

3.2 UHPFRC constitutive model

The elastic behaviour of concrete is specified by defining elastic modulus and Poisson's ratio assuming isotropic material before cracking occurs (refer to Table 2). Nonlinear behaviour of concrete has been defined using built-in Concrete Damage Plasticity (CDP) model available in ABAQUS. The yield surface of CDP model is a modified Drucker–Prager strength hypothesis [10]. The four input parameters that are required to fully describe the yield surface and flow rule include: dilation angle (ψ) in degrees, plastic flow potential eccentricity (ϵ), ratio of the strength in the biaxial state to the strength in the uniaxial state (σ_b/σ_o), and the shape factor that defines the yield surface in the deviatoric plane (K_c), are initially set to default values: 30º, 0.1, 1.16, and 0.67, respectively. Thereafter, parameters with significant influence on numerical results are calibrated based on experimental measurements.

Other parameters defining the behavior of UHPFRC are determined for uniaxial stress-strain curves. Figure 4 shows the uniaxial relationships implemented in CDP model side by side with tested uniaxial responses for both compression and tension. The uniaxial compressive stress-strain response of UHPFRC is modeled by fitting the experimental quasi-static curve with a piecewise linear model. The uniaxial tensile stress-strain response is elastic linear up to the tensile strength. The post-peak tension stiffening behavior is defined as stress-crack width response in order to minimize mesh dependency of numerical results. The fictitious crack model proposed by Hillerborg [11] is used to define the descending branch of uniaxial tensile stress-crack displacement based on the tensile fracture energy criterion. The model of strain hardening in tension is ignored because the fracture energy dissipated during strain hardening is very small (approximately 1%) in comparison to the dissipated energy during softening or fibres pull-out [2]. Damage is assumed to occur in the softening behavior in both compression and tension. The compression damage parameter (d_c) is simplified using a linear relationship. On the other hand, the tension damage (d_t) is defined using a bilinear model as illustrated in Figure 4-b.

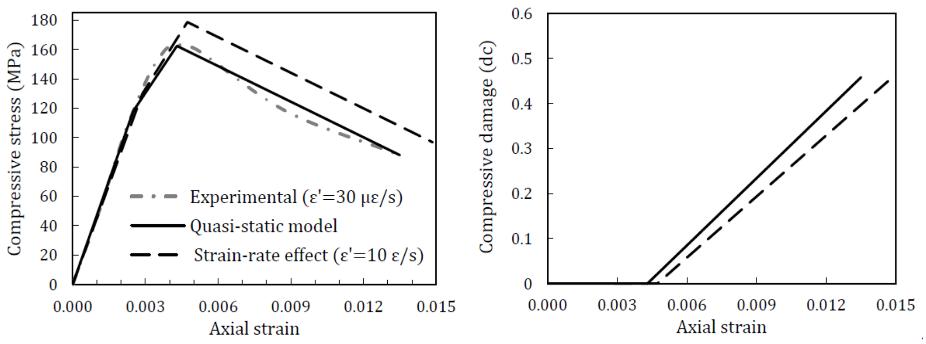

a) Compression input (left: stress-strain; right: damage)

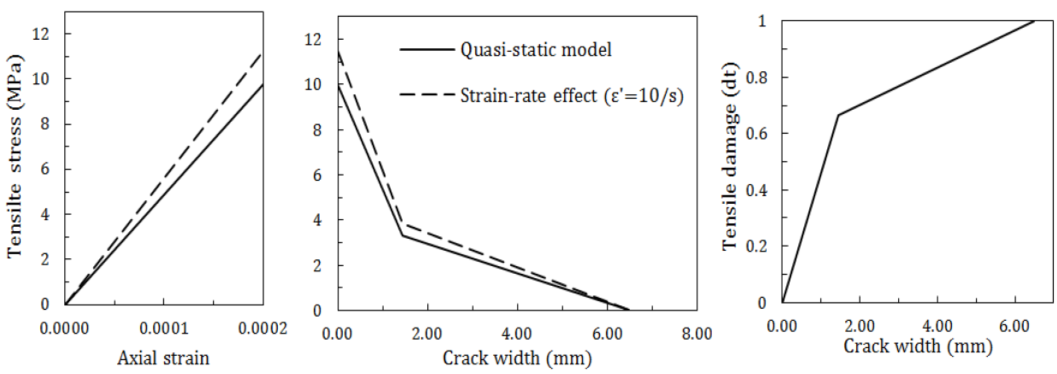

b) Tension input (left: stress-crack width; right: damage)

Figure 4: UHPFRC uniaxial relationships for concrete damage plasticity model

3.3 Steel reinforcement constitutive model

The classical metal plasticity model is used to define plastic behavior [6]. Figure 5 shows experimental and true stress-strain curves that are used to calculate the input of steel model. The strain rate effect in yield and ultimate strength are estimated using Malvar-Crawford model [12].

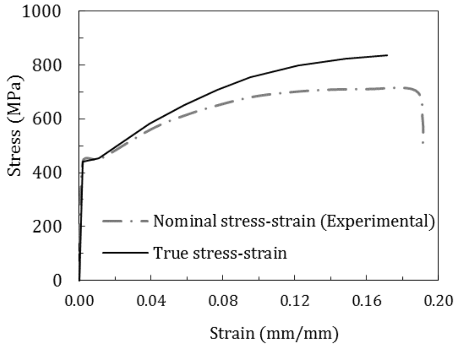

Figure 5: stress-strain curve of steel reinforcement

4. CALIBRATION OF CDP MODEL PARAMETERS

The FE model of UHPFRC is calibrated based on the results of the first impact test of specimen UH-S_{100}. Then, the predictive capability of calibrated model is checked by simulating the other two UHPFRC specimens with different reinforcement ratio. In the following analyses, the results of the FE models are compared to the experimentally measured impact force, reaction force, midpoint displacement, and steel strain gauge time histories. The time step for the explicit analysis is approximately 2 microseconds estimated automatically by ABAQUS/Explicit. The “restart analysis” option available in ABAQUS is used to define the new impact velocity of drop-weight and to allow the model continues using material properties from the termination point of previous analysis step in modeling consecutive impacts. A mesh size of 20 mm (5 elements through the thickness) is adapted to ensure the simulation produces a mathematical accurate solution.

As mentioned before, the input data of the CDP constitutive model are determined using the material data reported in Table 2 wherever possible. The parameters that cannot be determined directly from the available material measurements, including the uniaxial tensile strength, fracture energy, CDP parameters (ψ, ϵ, K_c, and σ_{bo}/σ_{co}), are selected based on a parametric study in which numerical results with assumed values for the parameters are matched with experimental measurements. Because of the lack of experimental data and proper formulas that defines UHPFRC behaviors, sensitivity analyses are performed first to quantify the influence of such input parameters on the numerical results. In these analyses, each parameter is varied over a large range of possible values and the findings are summarized in Table 3.

Table 3: Sensitivity analysis results

Material parameter	Significance	Material parameter	Significance
Tensile strength (f_t)	✓	Flow eccentricity (ϵ)	×
Fracture energy (G_F)	✓	Shape parameter (K_c)	×
Dilation angle (ψ)	✓	Ratio (σ_{bo}/σ_{co})	×
Poisson ratio (υ)	×	Damage (d_c, d_t)	✓

Based on the sensitivity analysis results, only the material parameters with significant effects are calibrated. CDP constitutive model parameters with high uncertainties, including fracture energy (G_F), uniaxial tensile strength (f_t) and dilation angle (ψ) are calibrated through a series of parametric studies using the experimental results of the first impact test of plate UH-S_{100}. Other CDP parameters with marginal effect, including ϵ, σ_{bo}/σ_{co}, K_c, and υ are set to the default values of 0.1, 1.16, 0.67, and 0.2 respectively. It was observed during the sensitivity analysis that the influences of material parameters on the impact force and reaction results are generally limited. Therefore, only the results of midpoint displacement and bottom steel strain at midpoint zone are considered.

In literature, UHPFRC of 140−180 MPa containing 1.5−2.5% short steel fibre by volume and cured under standard conditions, showed tensile fracture energies ranging from 14,000 to 21,000 N/m [13,14,2]. In this investigation, three different values of fracture energy (16,000, 18000, and 20000 N/m) with f_t = 10 MPa, and ψ = 30° are considered. Figure 6 illustrates the influence of the fracture energy on the computed responses. It is evident that the tension stiffening behavior of concrete has a pronounced effect on the impact response of the plate. Both midpoint displacement and steel strain are inversely proportional to the fracture energy value. Smaller fracture energy inputs indicate that the material has lower deformation capacity. It worth noting that ultimate localized crack width of UHPFRC is equal to half the fibre length (i.e., 6.5 mm) [2]. Based on the used fictitious crack model of Hillerborg [11], the maximum crack opening width corresponding to 20,000 N/m fracture energy is 7.2 mm in which over the theoretical crack opening capacity. On the other hand, the fracture energy of 18,000 N/m resulted in an ultimate maximum crack opening of 6.4 mm, close to the deformation capacity limit. Therefore, the fracture energy of 18,000 N/m is selected to be used in all the following analyses.

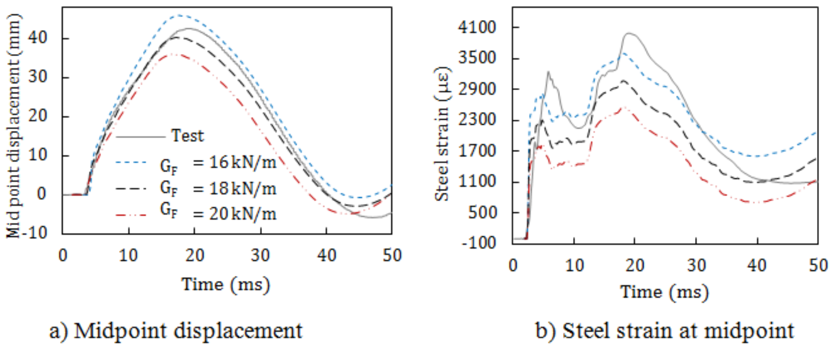

Figure 6: Influence of fracture energy

The tensile strength of UHPFRC has been measured using splitting tensile tests (see, Table 2). Thus, it is important to calibrate the estimated tensile strength. In this investigation, the uniaxial tensile strength variables in the range from 80 to 100 % of splitting tensile strength and the results are summarized in Figure 7. The tensile strength has limited effect on both computed displacement and steel strain responses. It might be because the considered tensile strength values are close to each other. In general, the uniaxial tensile strength of plain concrete is estimated as 90 % of concrete splitting strength [8]. Therefore, the uniaxial tensile strength is taken equal to 10 MPa same like conventional concrete.

Three different values of ψ (10°, 20°, 30°) with G_F = 18000 N/m, and f_t = 10 MPa are considered in this study. Figure 8 shows the influence of different values of dilation angle on the simulation results in comparison with experimental measurements. As shown, the simulation results of 10° dilation angle fit well with the experimental data. The selected dilation angle here is close to 15° which was adapted to model UHPFRC beam under static load using CDP model by Chen and Graybeal [15]. Such relatively small size of dilation angle is expected because UHPFRC has enhanced dense microstructure and exhibits less volume changes compared to conventional concrete.

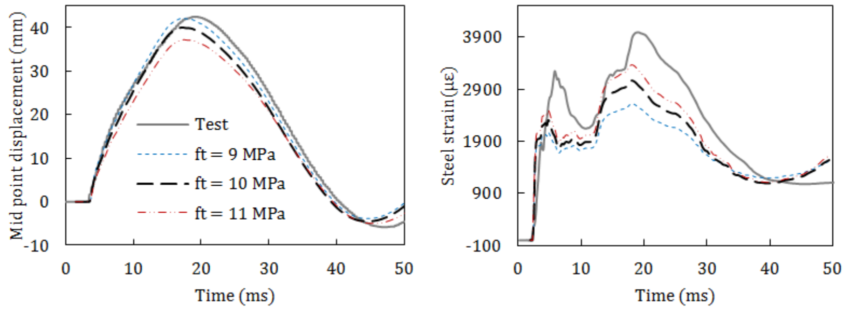

a) Midpoint displacement b) Steel strain at midpoint

Figure 7: Influence of tensile strength

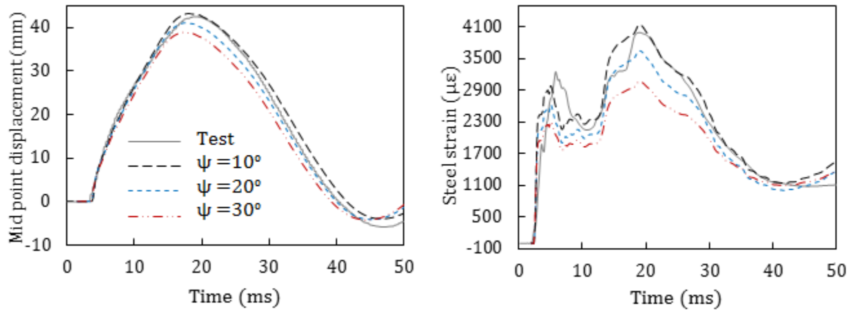

a) Midpoint displacement b) Steel strain at midpoint

Figure 8: Influence of dilation angle size

5. NUMERICAL RESULTS

This section presents the computed responses for the UHPFRC plates. The responses-time histories of UHPFRC plates under first impact tests are presented in Figure 9. The computed impact force-time, total reaction force-time, midpoint displacement-time, and steel strain-time histories are plotted alongside the test. It can be seen that the computed responses are in good agreement with experimental measurements in terms of peak values, time response, and overall shape. Similar levels of accuracy are obtained for second impact simulations as that attained in analyses of the first tests. The analytical results of the third and successive impacts showed less accurate estimates of the experimental responses. In general, the impact force and reaction are estimated with reasonable accuracy. On the other hand, the overall shape of the computed displacement and steel strain responses are found to significantly differ from the measured responses (Figure 10). The displacement and steel strain showed significant discrepancies in the form of larger time periods, unrecoverable response. Such differences in responses are mainly returned to the absence of modeling fibre contribution at microstructure level. This means that the CDP model can predict the dynamic response reasonably well for cases in which cracking is in the form of non-continuous micro-cracks in the cementitious paste. Therefore, an appropriate uniaxial tensile input model for UHP-FRC takes into account hardening and softening responses and the fracture energy is required. Such research would allow improvement, development, and generalization of numerical constitutive models.

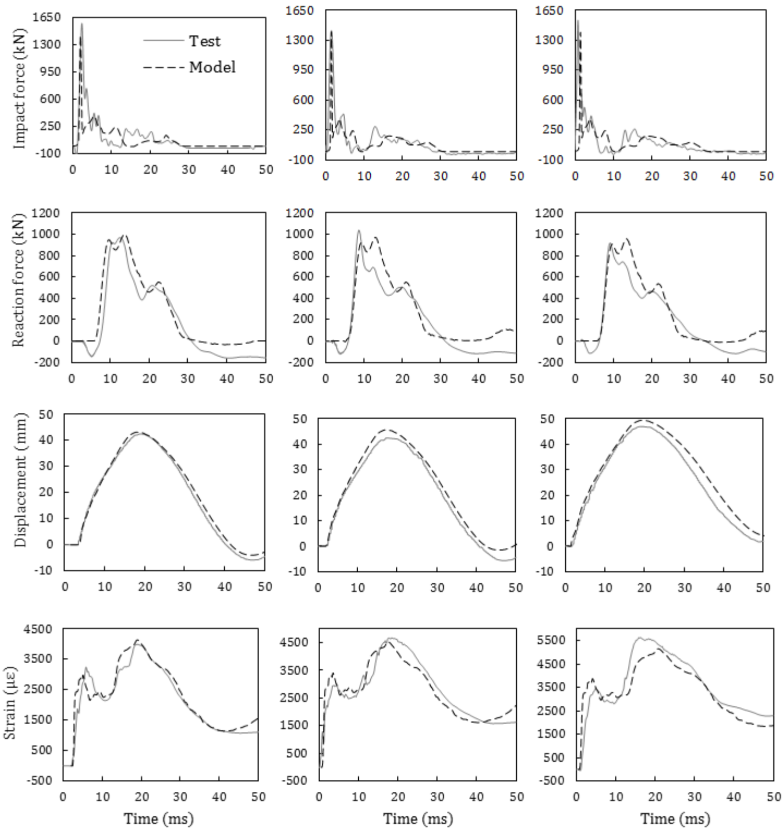

a) UH-S_{100} b) UH-S_{158} c) UH-S_{210}

Figure 9: Comparison of model prediction to test results of UHPFRC plates (1^{st} impact)

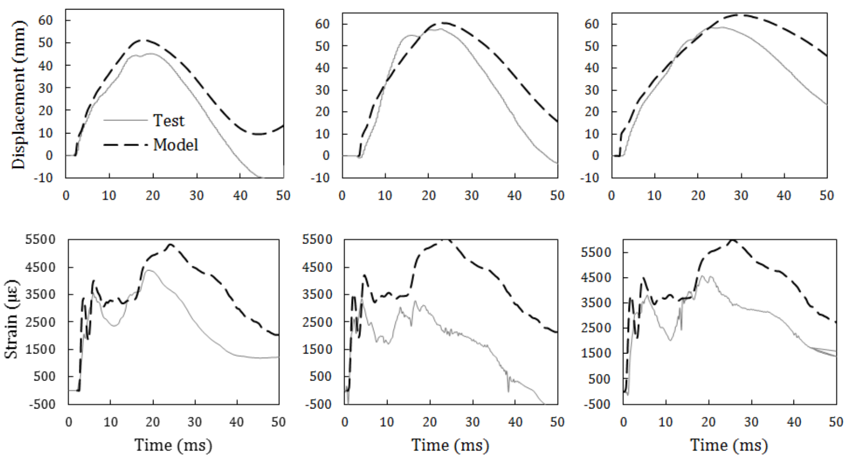

a) UH-S_{100} b) UH-S_{158} c) UH-S_{210}

Figure 10: Comparison of model prediction to test results of UHPFRC plates (3^{rd} impact)

6. CONCLUSIONS

The predicted responses of UHPFRC plates show promise with regards to model UHPFRC materials with the existing damage plasticity model. From the dynamic numerical study, the following conclusions are drawn:

- The computed dynamic response of UHPFRC was found to be significantly influenced by the fracture energy input than the uniaxial tensile strength value.
- Based on the numerical results, the plastic volume change of UHPFRC (dilation angle ≅ 10°) is small in comparison to traditional concrete (dilation angle ≅ 35°).

The numerical results of UHPFRC plates can demonstrate the feasibility of existing concrete damage plasticity constitutive model in estimating the dynamic response of new UHPFRC materials. However, instabilities of results were observed in the later-impact analyses that corresponding to damage level of fibres bridging action stage.

REFERENCES

[1] Wille, K., Kim, D. and Naaman, A., 'Strain-hardening UHP-FRC with low fiber contents', Mater. Struct. **44** (3) (2010) 583–598.

[2] Xu, M. and Wille, K., 'Fracture energy of UHP-FRC under direct tensile loading applied at low strain rates', Composites Part B: Engineering **80** (2015) 116–125.

[3] Wille, K., Naaman, A., El-Tawil, S. and Montesinos, G., 'Ultra-high performance concrete and fiber reinforced concrete: achieving strength and ductility without heat curing', Mater. Struct. **45** (3) (2011) 309–324.

[4] Toutlemonde, F., Boulay, C., Sercombe, J., Le Maou, F. and Renwez S., 'Characterization of reactive powder concrete (RPC) in direct tension at medium to high loading rates', in '2nd International Conference on Concrete under severe conditions : Environment and Loading', (1998), 887–896.

[5] Othman, H. and Marzouk, H., 'Strain rate sensitivity of fiber-reinforced cementitious composites', ACI Mater. J., **113** (2) (2016) 143–150.

[6] Simulia, 'ABAQUS 6.14 user's manuals'. Dassault Systèmes Simulia Corp (2016).

[7] CSA A23.3., 'Design of Concrete Structures', Canadian Standards Association, Mississauga - Canada (2004).

[8] CEB-FIP, 'Model code for concrete structures', International Federation for Structural Concrete (fib). Lausanne, Switzerland (2010).

[9] Othman, H. and Marzouk, H. 'Impact response of ultra-high-performance reinforced concrete plates', ACI Struct. J. **113** (6) (2016) 1325–1334.

[10] Lubliner, J., Oliver, J., Oller S. and Onate, E., 'A plastic-damage model for concrete', Solids Struct. **25** (1989) 299–326.

[11] Hillerborg A., 'The theoretical basis of a method to determine the fracture energy G_F of concrete', Mater. Struct. **18** (1985) 291–296.

[12] Malvar L, Crawford J., 'Review of static and dynamic properties of steel reinforcing bars', ACI Mater. J. **95** (1998) 609–616.

[13] Wille, K. and Naaman, A., 'Fracture energy of UHPFRC under direct tensile loading', in 'FraMCoS-7 international conference', Jeju, Korea: (2010).

[14] Voit K, Kirnbauer J. 'Tensile characteristics and fracture energy of fiber reinforced and non-reinforced ultra-high performance concrete (UHPC)', Int. J. Fract. **188** (2014) 147–157.

[15] Chen, L. and Graybeal, B., 'Modeling structural performance of ultrahigh performance concrete I-Girders', J. Brid. Eng. **17** (2011) 754–764.